Hybrid Polymer/Lipid Vesicles: Influence of polymer architecture and molar mass on line tension

Martin Fauquignon, Emmanuel Ibarboure, Jean-François Le Meins*

Université de Bordeaux, CNRS, Bordeaux INP, LCPO, UMR 5629, F-33600, Pessac, France.
lemeins@enscbp.fr

ABSTRACT: Hybrid polymer/lipid vesicles are self-assembled structures that have been the subject of an increasing number of studies in recent years. They are particularly promising tools in the development of cell membrane models as they offer the possibility to fine-tune their membrane structure by adjusting the distribution of components (presence or absence of "raft like" lipid domains) which is of prime importance to control their membrane properties. Line tension in multiphase membranes is known to be a key parameter on membrane structuration but remains unexplored, either experimentally or by computer modelling for hybrid polymer /lipid vesicles. In this study we were able to measure the line tension on different budded hybrid vesicles, using micropipette aspiration technique, and show the influence of the molar mass and the architecture of block copolymers on line tension and its consequences for membrane structuration.

Key words:

Hybrid Polymer lipid vesicles

Line tension

Micropipette aspiration

Condensed running title:

Line tension in hybrid vesicles

Statement of significance

Hybrid polymer/lipid vesicles with a membrane composed of phospholipids and amphiphilic copolymers are extremely promising structures for various fields of applications (drug delivery, development of nano-/micro-reactors, artificial cells, …). For all these applications a perfect control and knowledge of the membrane structure is essential. The line tension (energy per length unit) at the boundaries of polymer and lipid is a key parameter governing the membrane structure. However, this parameter is so far totally unknown for these

systems, hindering the optimization of their membrane properties. We report here the first experimental measurements of this parameter and clarify the role of the copolymer molar mass and architecture on the line tension and thus the membrane structure.

Introduction

Lipids are the major components of the cell membrane. In a bottom-up approach to understand cell function and behavior, phospholipids were the first synthetic molecules used to develop vesicles as a basic model of the cell membrane. Although more complex structures have been developed since then, for example by inserting membrane proteins or using different phospholipids to elaborate the membrane, these advanced structures remain short-lived, not very stable and without a natural mechanism of regeneration. In the late 1990s, polymersomes obtained by self-assembly of amphiphilic copolymers emerged as a potential replacement for phospholipids in the development of synthetic cells, due to their higher membrane toughness, chemical versatility and resistance.(1) In particular, they also allow the insertion of membrane proteins and grant them an extended functional lifetime.(2-4) More recently, hybrid polymer/lipid membranes have attracted great interest, as they can be considered as advanced vesicular structures compared to their forerunners (liposomes and polymersomes) as they harness the advantages of both components. The modulation of membrane properties between those of pure liposomes and polymersomes has indeed been observed, and generally speaking, these systems are of great interest to go further in the reproduction of dynamic biological phenomena. In particular, hybrid polymer/lipid systems tend to promote membrane fission and fusion for more efficient molecular trafficking(2). In most cases, the phenomenon result from the presence of a phase separation in the membrane, leading to polymer/lipid boundaries that exhibit a line tension, unquantified until now for such systems.

Line tension is defined as energy per unit length at boundaries in multiphase planar systems. It can be considered as the 1D analogue of the interfacial tension in 2D coexisting phases. The concept of line tension has been introduced to understand complex phenomena such as lateral phase separation, fusion, budding and fission in biological membranes,(5) which are essential for biological functions such as the production of transport vesicles, the presence of signaling domains in the membrane (existence of lipid raft), etc. Research in this area is particularly driven by the lively debate surrounding functionally important lipid/protein membrane inhomogeneities in living cells,(6, 7) and some applications such as the development of biomimetic bilayer sensors. Line tension has been shown to be one of the key parameters to modulate the shape, size and dynamics of the domains in a multiphase lipid bilayer membrane.(8, 9) Its experimental determination is tricky and relatively few values are reported in the literature for lipid bilayers. Baumgart and col. (10) determined the line tension through the shape of the domains observed by microscopy, using a shape theory previously developed by Julicher and Lipowsky.(11) Esposito and col. calculate the line tension from model boundary fluctuation in vesicles using domain flicker spectroscopy.(12) Honerkamp-smith et al. used the same approach to determine line tension in DPPC/diPhyPc/Cholesterol membranes.(13) Micropipette aspiration has also been used to measure line tension in Giant Unilamellar Vesicles (GUVs) with liquid ordered and liquid disordered phases.(14) Overall, the typical value is about a few picoNewtons for purely lipidic bilayers and can vary with the composition

of the membrane. So far, these variations have not been rationalized. However it has been shown that the line tension tends to decrease when the miscibility critical point is reached and increases when the thickness mismatch between the lipid phases increases.(15)

Hybrid polymer/lipid vesicles have emerged as self-assembled structures that spark an increasing interest from different scientific communities as promising objects for numerous application ares such such as controlled drug delivery, development of bioinspired micro-/nano-reactors, and functional membranes for artificial cells.(16, 17) However, despite an increasing number of studies, there is a lack of systematic approach that could decipher the molecular parameters necessary to control their membrane structuration and reach the desired membrane properties for a given application. Line tension has been discussed in direct analogy with a multicomponent lipid bilayer as a key parameter to control membrane structure. However, the experimental values of the line tension are unknown until now. The determination of the line tension in these hybrid vesicles is of prime importance to go further in the development of more complex and functional artificial cells. In this work, we designed different hybrid polymer/lipid vesicles from a mixture of 1-palmitoyl-2-oleoyl-glycero-3-phosphocholine (POPC) and poly(dimethylsiloxane)-b-poly(ethylene oxide) diblock or triblock copolymers (PDMS-b-PEO or PEO-b-PDMS-b-PEO), in a given lipid composition range. Besides the fact that these PDMS-based copolymers have already been used for the development of hybrid vesicles, they are also of great interest in synthetic biology for the development of artificial cells, as they have been shown to allow insertion of membrane protein in a functional state with an extended functional lifetime. Giant hybrid unilamellar vesicles (GHUVs) obtained with triblock copolymers present stable budded lipid domains, as demonstrated in a previous study.(18) These budded vesicles were also obtained with diblock copolymers,(19) allowing line tension measurement by the micropipette technique. We will show and discuss the importance of block copolymer architecture and hydrophobic length mismatch at the polymer/lipid boundaries on the line tension and the consequences in terms of membrane structuration.

Materials and Methods

All the copolymers used in this study were synthesised and fully characterized in previous work. (*18, 20*) The molecular characteristics of the copolymers as well as the membrane thicknesses of the polymersomes are indicated in Table 1. POPC, DOPC and 1,2-dioleoyl-sn-glycero-3-phosphoethanolamine-N-(lissamine rhodamine B sulfonyl) (DOPE-Rhod) were purchased from Sigma Aldrich and used without further purification.

Copolymer	^{1}H NMR in CDCl$_3$				SEC in THF	SANS
	Mn PDMS (g.mol^{-1})	Mn PEO (g.mol^{-1})	Mn copolymer (g.mol^{-1})	Hydrophilic fraction (%)	Dispersity Đ	Membrane Thickness* (nm)
PEO$_8$-*b*-PDMS$_{22}$-*b*-PEO$_8$ (*18*)	1628	350	2668	30	1.18	5.4 ± 0.4
PDMS$_{23}$-*b*-PEO$_{13}$ (*20*)	1700	600	2500	26	1.15	7.2 ± 0.8
PDMS$_{27}$-*b*-PEO$_{17}$ (*20*)	2000	700	2900	26	1.11	8.3 ± 1.1

Table 1. Molecular characteristics of the copolymers used in this study. * data from(20, 21) Mn is the average molar mass in number.

GHUVs' Preparation

Giant unilamellar vesicles were prepared at room temperature using the electro-formation protocol reported by Angelova[22]. Briefly, solutions containing the appropriate amount of copolymer and POPC were solubilized in chloroform at 1 mg.ml^{-1}. Then, 50 µl of the solution were spread on ITO glass plates. Traces of chloroform were removed under vacuum during at least 3 hours. Next, the ITO glass plates were sealed together to form the electro-formation chamber, connected to an AC voltage and filled with a 100mM sucrose solution. A sinusoidal tension (2 V, 10 Hz) was applied during 75 min for all systems used. For the identification of polymer and lipid phases in GHUVs, fluorescent probes were used : PDMS-nitrobenzoxadiazole (PDMS-NBD) (1 mol.%) for polymer phases (synthesis protocol is available in[20]) and 1,2-dioleoyl-sn-glycero-3-phosphoethanolamine-N-(lissamine rhodamine B sulfonyl) (DOPE-Rhod) at 0.1 mol.% for lipid phases.

The micropipette-aspiration experiment

The micropipette-aspiration experiment was carried out using a Leica TCS SP5 (Leica Microsystems CMS GmbH, Mannheim, Germany) inverted confocal microscope (DMI6000) equipped with an x63 apochromatic water immersion objective with an NA of 1.2 (Zeiss, Jena, Germany). Micropipettes were obtained by stretching Borosilicate capillaries (1 mm OD, 0.58 mm ID) from WPI, using a pipette puller (Sutter Instrument P-97, Novato, USA). The pulled pipettes were then forged into the desired diameter using a Narishige MF-900 micro-forge (London, U.K). The micropipettes were coated with BSA to prevent vesicle adhesion. GUVs were injected and allowed to sediment in a glucose meniscus formed between two glass slides glued to a home-made aluminium microscope stage. Vesicle tension was controlled using a home-made hydraulic water-tight setup. The micropipette was controlled using a micromanipulator (Eppendorf, Patchman NP2, Montesson , France).

The suction pressure exerted over the membrane can be calculated from:

$$\Delta P = (h - h_0)\, \rho\, g \tag{1}$$

where ρ is the water density, g is the gravitational acceleration, h is the position of the water tank and h_0 is the initial position where the pressure is zero.

The membrane tension was classically calculated using the Laplace equation:

$$\sigma = \frac{\Delta P}{2} \frac{R_p}{\left(1 - \frac{R_p}{R_v}\right)} \tag{2}$$

where R_P and R_V are respectively the micropipette and the vesicle radii (outside the micropipette), and DP is the suction pressure.

The relative area change of the membrane α is defined as:

$$\alpha = \frac{A - A_0}{A_0} \tag{3}$$

where A_0 is the membrane area of the vesicle at the lower suction pressure. α can be estimated from the increase in projection length ΔL of the vesicle inside the capillary tip according to the following:

$$\alpha = \frac{1}{2} \left(\frac{R_P}{R_V}\right)^2 \left(1 - \frac{R_P}{R_V}\right) \frac{\Delta L}{R_P} \tag{4}$$

The surface area strain can be linked to the membrane tension through the following equation:

$$\alpha = \frac{k\,T}{8\,\pi\,K_b} \ln\left(1 + \frac{A_0\,\sigma}{24\,\pi\,K_b}\right) + \frac{\sigma}{K_a} \tag{5}$$

Where k is the Boltzmann constant, T the temperature and Kb and Ka respectively the bending and stretching modulus. The Kb can be extracted from the slope of the curve $Ln(\sigma)$ versus α, at a low tension regime (typically up to $\alpha = 1\%$) where the surface area increase is almost entirely due to damping of thermal shape fluctuations, in other words, bending undulations in the bilayer.[23-28]

Results and discussion

In a previous study, we established an apparent phase diagram of GHUV membrane structuration obtained from the mixture of POPC and triblock copolymer $PEO_8\text{-}b\text{-}PDMS_{22}\text{-}b\text{-}PEO_8$.(18) In a given compositional range, stable budded vesicles were obtained, with each hemisphere being formed by either the polymer phase or the lipid phase. Figure 1 illustrates budded vesicles under micropipette suction.
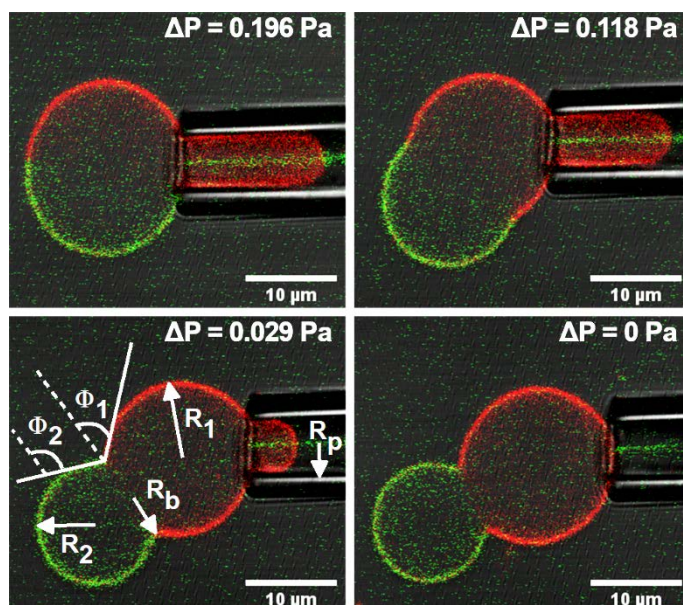
Figure 1. Example of line tension measurement on GHUVs made from PDMS$_{23}$-b-PEO$_{13}$/POPC at different suction pressure (values indicated in the top right of each picture). Lipid phases are tagged in red while polymer phases are tagged in green.

This morphology reflects a budding-fission process that was stopped through a balance between the boundary energy and the bending cost of energy. This phenomenon was also observed with diblock copolymers PDMS$_{27}$-b-PEO$_{17}$ and PDMS$_{23}$-b-PEO$_{13}$ when forming GHUVs.(*29*) This particular shape of GHUVs can provide insight into the boundary energy between the polymer and the lipid phases, also known as line tension. In Figure 2, a schematic of the hybrid polymer/lipid membrane with lateral phase separation is shown for clarification.
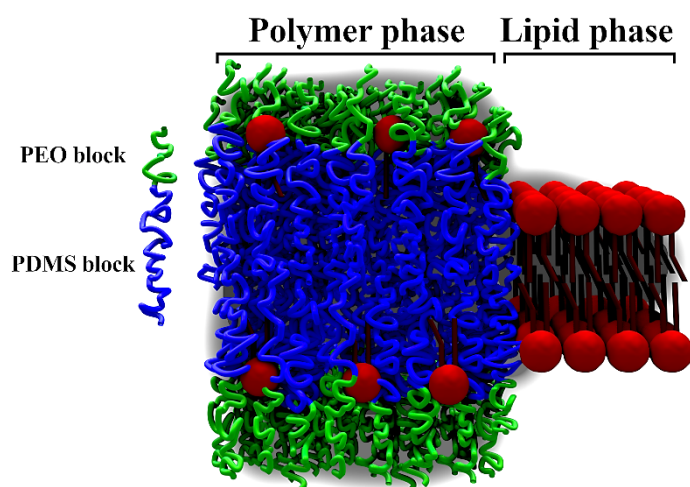

Figure 2: Schematic view of the Hybrid polymer/lipid membrane with a lateral phase separation.

We used a model developed by Baumgart *and col.*(*14*) to extract the line tension from micropipette measurements performed on GHUVs made from diblock or triblock copolymers. First, the bending moduli K$_b$ of the different polymersomes were evaluated to verify whether the bending energy can indeed be neglected compared to the boundary energy. The corresponding experimental curves are shown in Figure 3. We obtained for the polymersomes made from the diblock copolymers PDMS$_{27}$-b-PEO$_{17}$ and PDMS$_{23}$-b-PEO$_{13}$ bending moduli of 10.0 ± 1.6 kT and 10.1 ± 3.4 kT, respectively. Bending modulus of polymersomes made from triblock copolymers PEO$_8$-b-PDMS$_{22}$-b-PEO$_8$ was slightly higher, with an average value of 12.7 ± 2.9 kT. Because the measurement of bending moduli and line tension involves the use of very low suction pressure, we verified the accuracy of our experimental setup and procedure, by measuring bending modulus of GUVs made from DOPC (data available in supporting information). We obtained a bending modulus of 10.9 ± 0.8 kT, in reasonable agreement with the value of 11.7 ± 1.5 kT obtained in literature (*30, 31*) by micropipette aspiration for similar sucrose concentration. We can therefore consider our data to be reliable.

The values obtained for the three copolymers are in the same range than DOPC[26,27] and lower than what is observed for POPC.(*26, 28*). They are also significantly lower than the bending moduli reported for polymersomes made from coil-coil block copolymers,(*23*) with comparable

membrane thicknesses (~7-9 nm). As the PDMS chains in the membrane has also been shown to exhibit a coil conformation (membrane thickness scales with $M\sim^{0.52}$)[20], this may be related to the high fluidity for such molar mass due to their low Tg (~ -120°C) and high critical entanglement molar mass (~30.000 g.mol^{-1}). Similar values of K_b were observed for both diblock copolymers, despite a slight but noticeable difference in membrane thickness. The relatively high uncertainty of such measurements probably prevent to see the expected effect of the membrane thickness. The variation in length of the hydrophobic block is not very high (only 4 units between the two diblock copolymers). As K_b scales as d^2,[23] and d scales as $M^{\sim0.52}$, Kb should scale as $M^{\sim1.3}$. This may be the case but we cannot confirm it regarding the size of the error bars. However, it is interesting to note that in literature K_b of large unilamellar vesicles (LUVs) of $PDMS_{60}$-b-$PMOXA_{21}$ has been measured at 25 kT.[32] Considering the value of ~10 kT for polymersomes made of $PDMS_{27}$, a reasonable agreement is found with the literature value. Indeed, assuming a scaling law of $K_b \sim M^{1.3}$, a value of 28 kT should be obtained for $PDMS_{60}$, which is very close to what has been observed.
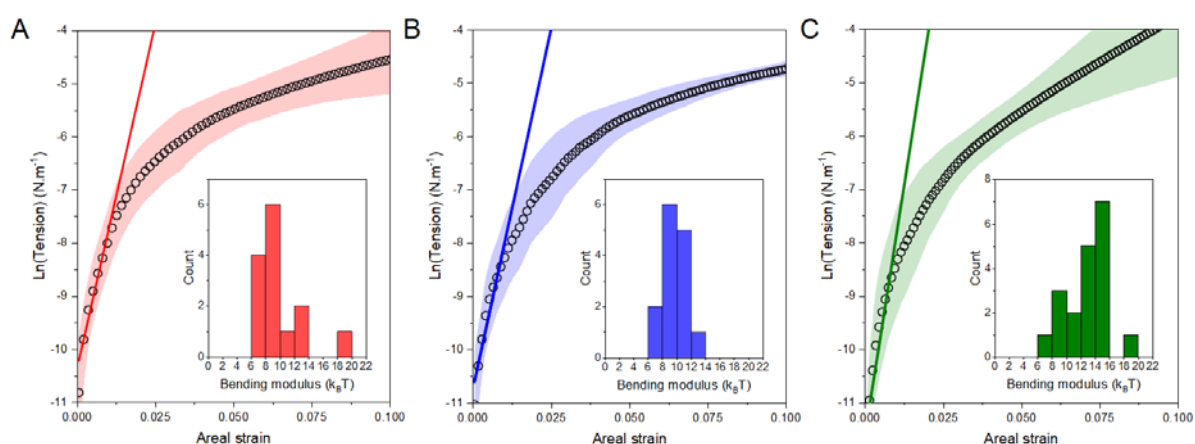
Figure 3. Average measurements (black circles) and standard deviation (colored areas) of the membrane tension as a function of areal strain for the polymersomes obtained from $PDMS_{23}$-b-PEO_{13} (A), $PDMS_{27}$-b-PEO_{17} (B) and PEO_8-b-$PDMS_{22}$-b-PEO_8 (C). Bending moduli are extracted from the slope of the curve (linear regression) in the low-tension regime.

Line tension was determined by measuring the geometric factor of the vesicles at different suction pressures. We used a model developed by Baumgart and col.[14] based on the analysis of the shape of budded vesicles during their deformation. Basically, the two meridional tangent angles ϕ_1 and ϕ_2 of the lipid and polymer phases, as well as the boundary and pipette radius R_b and R_p are considered (see Figure 1). The evolution of R_b, ϕ_1 and ϕ_2 with the suction pressure ΔP is measured. The thermo-mechanical equilibrium of the budded vesicle is assumed to depend mainly on the lateral tension, the suction pressure ΔP, the vesicle normal pressure difference outside the pipette and the line tension λ. The bending-stiffness contribution is neglected, assuming that the boundary energies are significantly higher than the bending energy.[33] The line tension λ can be linearly related to ΔP and a geometric factor A as follows:

$$\lambda = \Delta P \frac{R_b^2 R_p \sin\phi_1}{2(R_b - R_p \sin\phi_1)}(\cot\phi_1 - \cot\phi_2) = \Delta P \, A \qquad (6)$$

The boundary energy was estimated assuming a typical value found in a lipid bilayer membrane for the line tension λ (~1 pN) and a radius of the circular boundary R_b of 10 µm. This gives a boundary energy of $E_b \sim 2\pi\lambda R_b \sim 6.10^{-17}$ J, which is higher than the bending energy for a membrane ($\sim 8\pi K_b$): $\sim 1.10^{-18}$ J. This confirms the validity of the assumption made in the model used. A more detailed comment about these calculations is available in supporting information.

The line tension measurements were carried out using the micropipette set-up described previously. 10 µl of the vesicle suspension was injected in the glucose meniscus before surrounding the meniscus with mineral oil to prevent water evaporation. After 15 minutes of sedimentation, vesicles deposited at the bottom. The GHUVs showing budding with strong angles were selected. The pipette was gently lowered and approached the lipid-rich side of the membrane with low suction pressure. The pressure was increased to create a significant projection length inside the pipette until the budding disappears. From this position, the pressure was reduced to restore the budded structure. A series of 3 to 8 images was recorded at different suction steps. The zero pressure was corrected to correspond to the stage where the length projection was no longer visible. From the recorded images, some characteristic dimensions were measured such as the radius at the budding boundary R_b, the radius of the pipette R_p, and the meridional tangent angles Φ_1 and Φ_2. These parameters are linked to the line tension according to Eq. 6. The inverse of the parameter A was plotted as a function of the suction pressure ΔP (figure 4), allowing the line tension to be calculated from the slope of the linear part.
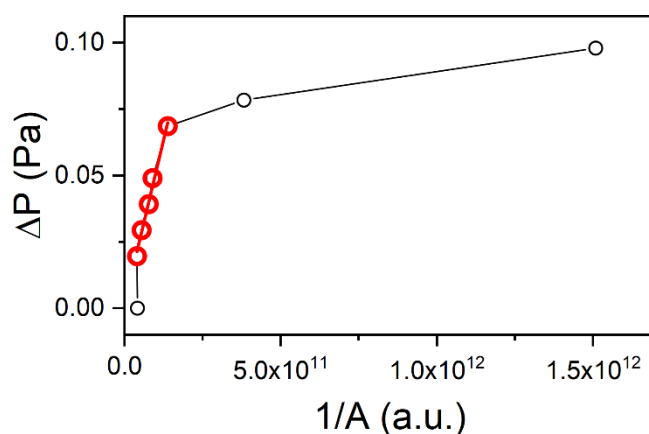

Figure 4. Example of the evolution of the suction pressure as a function of the geometrical parameter (1/A) for the hybrid system POPC/PEO$_8$-b-PDMS$_{22}$-b-PEO$_8$. The red part corresponds to a linear evolution whose slope allow to determine the line tension.

This experiment was carried out on GHUVs with a POPC content of 50 wt.%. Measurements were performed on 10 budded vesicles for PDMS$_{23}$-b-PEO$_{13}$, 16 vesicles for PDMS$_{27}$-b-PEO$_{17}$ and 13 vesicles for PEO$_8$-b-PDMS$_{22}$-b-PEO$_8$.

The line tension values are obtained with a relatively high uncertainty, as it is commonly observed for such measurements (Figure 5). Calculation of relative error inherent to the experimental procedure on the line tension, as well as statistical tests, were performed to found out significance of the line tension difference between all systems. All these informations are available in supporting information. We can see that for diblock copolymers, an increase in the hydrophobic length mismatch leads to an increase in the line tension. This result is in agreement

with theoretical simulations (15) and observations in multiphase liposomes.(34) The values are in the order of what is observed for multiphase lipid bilayer membranes,(9, 14) which at first sight can be quite surprising: the compatibility between dimethylsiloxane monomer and alkyl tail is lower than that between alkyl tails of different lipids. Indeed, the solubility parameter of PDMS is $\delta = 7.3$ cal$^{1/2}$/cm$^{3/2}$,(35, 36) while that of the fatty acid tails in phospholipids is $\delta = 9.1$ cal$^{1/2}$/cm$^{3/2}$. It is worth mentioning that the lipid is able to diffuse into the polymer phase to some extent.(21) This may contribute to reduce the incompatibility between the two phases and thus the line tension.

Another interesting observation is that the line tension for PEO$_8$-b-PDMS$_{22}$-b-PEO$_8$ is slightly higher than for PDMS$_{23}$-b-PEO$_{13}$ despite a slightly lower hydrophobic length mismatch. In fact, its line tension is closer to that of PDMS$_{27}$-b-PEO$_{17}$ whereas they have almost 3 nm difference in hydrophobic length mismatch. This suggests that the adaptation between the polymer and the lipid at the boundaries depends on the architecture of the copolymer used. It has been established in literature that diblock copolymers exhibit exclusively a loop conformation, ensuring a bilayer membrane, while a mixture of extended conformation and loop is observed in membrane composed of triblock copolymers. (37, 38) These conformational differences may be the cause of a less efficient chain adaptation at the polymer/lipid boundaries.

Finally, this could explain the differences in phase diagrams that have been established in previous studies for GHUVs obtained with a mixture of POPC and these diblock and triblock copolymers. (18, 19) For example, for a same lipid composition of 30 wt.% a majority of GHUVs made from triblock copolymers PEO$_8$-b-PDMS$_{22}$-b-PEO$_8$ show micrometer-size domains whereas only 10% of the GHUVs present a phase separation in the case of diblock PDMS$_{23}$-b-PEO$_{13}$.(18, 19) Given the higher line tension for PEO$_8$-b-PDMS$_{22}$-b-PEO$_8$/POPC, the system tends to form lipid microdomains more easily when increasing the lipid fraction. These domains are formed by the coalescence of nanodomains, in analogy to what has been observed with multiphase lipid vesicles,(39) to limit the boundary energy cost. For higher hydrophobic length mismatch, both triblock and diblock copolymers do not form hybrid vesicles with micrometric lipid domains. The incompatibility and the line tension (although not measurable in this case) are probably too high. Above a given lipid fraction, only liposomes and polymersomes (containing a small amount of lipid) are formed, resulting from a fast budding fission process.
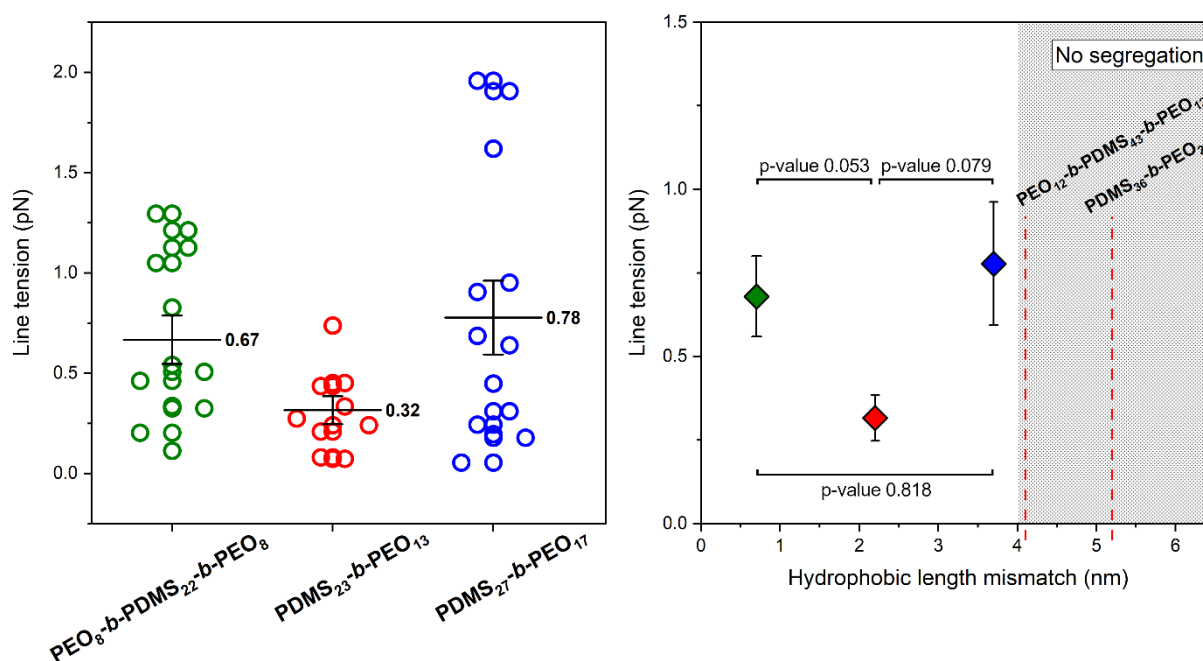
Figure 5. Left: Scatter plot of measurements obtained for $PDMS_{23}$-b-PEO_{13}/POPC (red dots), $PDMS_{27}$-b-PEO_{17}/POPC (blue dots) and PEO_8-b-$PDMS_{22}$-b-PEO_8/POPC (green dots) (Data: Mean (value indicated) ± SEM). Right: Evolution of the line tension as a function of the hydrophobic length mismatch (Data: Mean ± SEM (Standard Error of Mean); Brown-Forsythe and Welch test; Games-Howell's multiple comparisons post-test). The red dotted line in the shaded area corresponds to the thickness mismatch for other copolymers, for which hybrid vesicles were obtained without lateral phase separation whatever the lipid composition.

Conclusion

In this work, we reported the first experimental measurements of line tension in hybrid polymer/lipid vesicles. The values are in the range of what is observed for multiphase lipid vesicles. This explains why such structures can be obtained relatively easily, which was not obvious until recently. In addition to the hydrophobic length mismatch effect, the effect of the block copolymer architecture is important on the line tension, and consequently on the membrane structuration of these hybrid vesicles. This information is essential for the development of this type of synthetic cells where control of the transport of molecules across the membrane is a challenge. The determination of the line tension in polymer/lipid hybrid systems is an important step towards a better understanding of the structure and properties of hybrid membrane. This will make it possible in the future to design of functional artificial cells based on complex mixtures of polymers and lipids.

REFERENCES

1.   Rideau, E., R. Dimova, P. Schwille, F. R. Wurm, and K. Landfester. 2018 Liposomes and polymersomes: a comparative review towards cell mimicking, Chem Soc Rev 47, 8572-8610. doi: 10.1039/c8cs00162f

2.   Marušič, N., L. Otrin, Z. Zhao, R. B. Lira, F. L. Kyrilis, F. Hamdi, P. L. Kastritis, T. Vidaković-Koch, I. Ivanov, K. Sundmacher, and R. Dimova. 2020 Constructing artificial respiratory chain in polymer compartments: Insights into the interplay between bo3 oxidase and the membrane, Proc. Natl. Acad. Sci. 117, 15006. doi: 10.1073/pnas.1919306117

3.   Kleineberg, C., C. Wolfer, A. Abbasnia, D. Pischel, C. Bednarz, I. Ivanov, T. Heitkamp, M. Borsch, K. Sundmacher, and T. Vidakovic-Koch. 2020 Light-Driven ATP Regeneration in Diblock/Grafted Hybrid Vesicles, Chembiochem. doi: 10.1002/cbic.201900774

4.   Itel, F., A. Najer, C. G. Palivan, and W. Meier. 2015 Dynamics of Membrane Proteins within Synthetic Polymer Membranes with Large Hydrophobic Mismatch, Nano Lett. 15, 3871-3878. doi: 10.1021/acs.nanolett.5b00699

5.   Yang, S.-T., V. Kiessling, and L. K. Tamm. 2016 Line tension at lipid phase boundaries as driving force for HIV fusion peptide-mediated fusion, Nat. Commun. 7, 11401. doi: 10.1038/ncomms11401

6.   Munro, S. 2003 Lipid rafts: elusive or illusive?, Cell 115, 377-388. doi: S0092867403008821 [pii]10.1016/s0092-8674(03)00882-1

7.   Levental, I., K. R. Levental, and F. A. Heberle. 2020 Lipid Rafts: Controversies Resolved, Mysteries Remain, Trends Cell Biol. 30, 341-353. doi: 10.1016/j.tcb.2020.01.009

8.   Garcia-Saez, A. J., S. Chiantia, and P. Schwille. 2007 Effect of line tension on the lateral organization of lipid membranes, J. Biol. Chem. 282, 33537-33544.

9.   Usery, R. D., T. A. Enoki, S. P. Wickramasinghe, M. D. Weiner, W.-C. Tsai, M. B. Kim, S. Wang, T. L. Torng, D. G. Ackerman, F. A. Heberle, J. Katsaras, and G. W. Feigenson. 2017 Line Tension Controls Liquid-Disordered + Liquid-Ordered Domain Size Transition in Lipid Bilayers, Biophys. J. 112, 1431-1443. doi: 10.1016/j.bpj.2017.02.033

10.   Baumgart, T., S. T. Hess, and W. W. Webb. 2003 Imaging coexisting fluid domains in biomembrane models coupling curvature and line tension, Nature 425, 821-824. doi: 10.1038/nature02013 nature02013 [pii]

11.   Jülicher, F., and R. Lipowsky. 1996 Shape transformations of vesicles with intramembrane domains, Physical Review E 53, 2670-2683. doi: 10.1103/PhysRevE.53.2670

12.   Esposito, C., A. Tian, S. Melamed, C. Johnson, S.-Y. Tee, and T. Baumgart. 2007 Flicker spectroscopy of thermal lipid bilayer domain boundary fluctuations, Biophys. J. 93, 3169-3181. doi: 10.1529/biophysj.107.111922

13.   Honerkamp-Smith, A. R., P. Cicuta, M. D. Collins, S. L. Veatch, M. den Nijs, M. Schick, and S. L. Keller. 2008 Line Tensions, Correlation Lengths, and Critical Exponents in Lipid Membranes Near Critical Points, Biophys. J. 95, 236-246. doi: 10.1529/biophysj.107.128421

14.   Tian, A., C. Johnson, W. Wang, and T. Baumgart. 2007 Line Tension at Fluid Membrane Domain Boundaries Measured by Micropipette Aspiration, Phys. Rev. Lett. 98, 208102. doi: 10.1103/PhysRevLett.98.208102

15.   Kuzmin, P. I., S. A. Akimov, Y. A. Chizmadzhev, J. Zimmerberg, and F. S. Cohen. 2005 Line tension and interaction energies of membrane rafts calculated from lipid splay and tilt, Biophys J 88, 1120-1133. doi: S0006-3495(05)73181-7 [pii]10.1529/biophysj.104.048223

16.   Schulz, M., and W. H. Binder. 2015 Mixed Hybrid Lipid/Polymer Vesicles as a Novel Membrane Platform, Macromol. Rapid Comm. 36, 2031–2041. doi: 10.1002/marc.201500344

17.   Le Meins, J. F., C. Schatz, S. Lecommandoux, and O. Sandre. 2013 Hybrid polymer/lipid vesicles: state of the art and future perspectives, Mater. Today 16, 397–402.

18.   Dao, T. P. T., F. Fernandes, E. Ibarboure, K. Ferji, M. Prieto, O. Sandre, and J.-F. Le Meins. 2017 Modulation of phase separation at the micron scale and nanoscale in giant polymer/lipid hybrid unilamellar vesicles (GHUVs), Soft Matter 13, 627-637. doi: 10.1039/c6sm01625a

19.   Fauquignon, M., E. Ibarboure, and J.-F. Le Meins. 2021 Membrane reinforcement in giant hybrid polymer lipid vesicles achieved by controlling the polymer architecture, Soft Matter 17, 83-89. doi: 10.1039/d0sm01581d

20.   Fauquignon, M., E. Ibarboure, S. Carlotti, A. Brûlet, M. Schmutz, and J.-F. Le Meins. 2019 Large and Giant Unilamellar Vesicle(s) Obtained by Self-Assembly of Poly(dimethylsiloxane)-b-poly(ethylene oxide) Diblock Copolymers, Membrane Properties and Preliminary Investigation of their Ability to Form Hybrid Polymer/Lipid Vesicles, Polymers 11, 2013.

21.   Dao, T. P. T., A. Brûlet, F. Fernandes, M. Er-Rafik, K. Ferji, R. Schweins, J. P. Chapel, A. Fedorov, M. Schmutz, M. Prieto, O. Sandre, and J. F. Le Meins. 2017 Mixing Block Copolymers with Phospholipids at the Nanoscale: From Hybrid Polymer/Lipid Wormlike Micelles to Vesicles Presenting Lipid Nanodomains, Langmuir 33, 1705-1715. doi: 10.1021/acs.langmuir.6b04478

22.   Angelova, M. I., and D. S. Dimitrov. 1986 Liposome electroformation, Faraday Discuss. Chem. Soc. 81, 303-311.

23.   Bermudez, H., D. A. Hammer, and D. E. Discher. 2004 Effect of Bilayer Thickness on Membrane Bending Rigidity, Langmuir 20, 540-543.

24.   Evans, E., and W. Rawicz. 1990 Entropy-driven tension and bending elasticity in condensed-fluid membranes, Phys. Rev. Lett. 64, 2094-2097.

25.   Fa, N., C. Marques, E. Mendes, and A. Schröder. 2004 Rheology of giant vesicles: a micropipette study, Phys Rev Lett. 92, 108103-108101 108103-108104.

26.   Dimova, R. 2014 Recent developments in the field of bending rigidity measurements on membranes, Adv. Colloid Interface Sci. 208, 225-234. doi: 10.1016/j.cis.2014.03.003S0001-8686(14)00103-1 [pii]

27.   Ly, H. V., D. E. Block, and M. L. Longo. 2002 Interfacial Tension Effect of Ethanol on Lipid Bilayer Rigidity, Stability, and Area/Molecule: A Micropipet Aspiration Approach, Langmuir 18, 8988-8995. doi: 10.1021/la026010q

28.   Rawicz, W., K. C. Olbrich, T. McIntosh, D. Needham, and E. Evans. 2000 Effect of chain length and unsaturation on elasticity of lipid bilayers, Biophys. J. 79, 328-339.

29.   Fauquignon, M., E. Ibarboure, and J.-F. Le Meins. 2020 Membrane reinforcement in giant hybrid polymer lipid vesicles achieved by controlling the polymer architecture, Soft Matter. doi: 10.1039/d0sm01581d

30.   Nagle, J. F., M. S. Jablin, S. Tristram-Nagle, and K. Akabori. 2015 What are the true values of the bending modulus of simple lipid bilayers?, Chemistry and Physics of Lipids 185, 3-10. doi: 10.1016/j.chemphyslip.2014.04.003

31.   Shchelokovskyy, P., S. Tristram-Nagle, and R. Dimova. 2011 Effect of the HIV-1 fusion peptide on the mechanical properties and leaflet coupling of lipid bilayers, New J Phys 13, 25004-25004. doi: 10.1088/1367-2630/13/2/025004

32.   Winzen, S., M. Bernhardt, D. Schaeffel, A. Koch, M. Kappl, K. Koynov, K. Landfester, and A. Kroeger. 2013 Submicron hybrid vesicles consisting of polymer-lipid and polymer-cholesterol blends, Soft Matter 9, 5883-5890. doi: 10.1039/c3sm50733e

33.   Allain, J.-M., and M. Ben Amar. 2006 Budding and fission of a multiphase vesicle, The European Physical Journal E 20, 409-420. doi: 10.1140/epje/i2006-10030-4

34.   Blanchette, C. D., W.-C. Lin, C. A. Orme, T. V. Ratto, and M. L. Longo. 2008 Domain nucleation rates and interfacial line tensions in supported bilayers of ternary mixtures containing galactosylceramide, Biophys. J. 94, 2691-2697. doi: 10.1529/biophysj.107.122572

35.   Roth, M. 1990 Solubility parameter of poly(dimethyl siloxane) as a function of temperature and chain length, J. Polym. Sci. B. 28, 2719.

36.   King, J. W. 2002 Supercritical fluid technology for lipid extraction, fractionation and reactions, In Lipid biotechnology (Kuo, T. M., and Gardner, H. W., Eds.), pp 663-687, Marcel Dekker, New York.

37.   Itel, F., M. Chami, A. Najer, S. Loercher, D. Wu, I. A. Dinu, and W. Meier. 2014 Molecular Organization and Dynamics in Polymersome Membranes: A Lateral Diffusion Study, Macromolecules 47, 7588-7596. doi: 10.1021/ma5015403

38.   Tsai, H.-C., Y.-L. Yang, Y.-J. Sheng, and H.-K. Tsao. 2020 Formation of Asymmetric and Symmetric Hybrid Membranes of Lipids and Triblock Copolymers, Polymers 12, 639.

39.   Heberle, F. A., R. S. Petruzielo, J. Pan, P. Drazba, N. Kucerka, R. F. Standaert, G. W. Feigenson, and J. Katsaras. 2013 Bilayer Thickness Mismatch Controls Domain Size in Model Membranes, J. Am. Chem. Soc. 135 6853–6859. doi: 10.1021/ja3113615

Supporting Information.

Protocol to perform micropipette aspiration.

AUTHOR INFORMATION

Corresponding Author

Jean-François Le Meins lemeins@enscbp.fr

Author Contributions

Martin Fauquignon: Experiments and data analysis. Emmanuel Ibarboure: experiments and data analysis. JF Le Meins: Funding acquisition, research orientation, methodology, writing manuscript

SUPPLEMENTAL INFORMATION FOR:

Hybrid Polymer/Lipid Vesicles: Influence of polymer architecture and molar mass on line tension

Martin Fauquignon, Emmanuel Ibarboure, Jean-François Le Meins*

Université de Bordeaux, CNRS, Bordeaux INP, LCPO, UMR 5629, F-33600, Pessac, France.
lemeins@enscbp.fr

Measurement of Kb on DOPC Giant vesicle.

Kb was measured on Giant DOPC vesicle to check the accuracy of our experimental set up for very low succion pressure that are applied for Kb and Line tension measurement. 11 vesicles were analysed. Results are indicated in Figure S 1 and S2. we obtained a bending modulus of 10.4±2.5kT, from the average of bending moduli obtained by fitting each curves. The fit of the average curve, indicated on figure S2, give 10.9±0.8kT. The fit takes into account the experimental points up to 0.01 of the areal strain to ensure that it is in the low tension (fluctuation) regime. All Kb in this article were measured with this methodology.

Figure S1: Ln(tension) versus areal strain for DOPC vesicle. The experimental curve plotted correspond to the average of all experiments and grey shaded area correspond to the standard deviation.
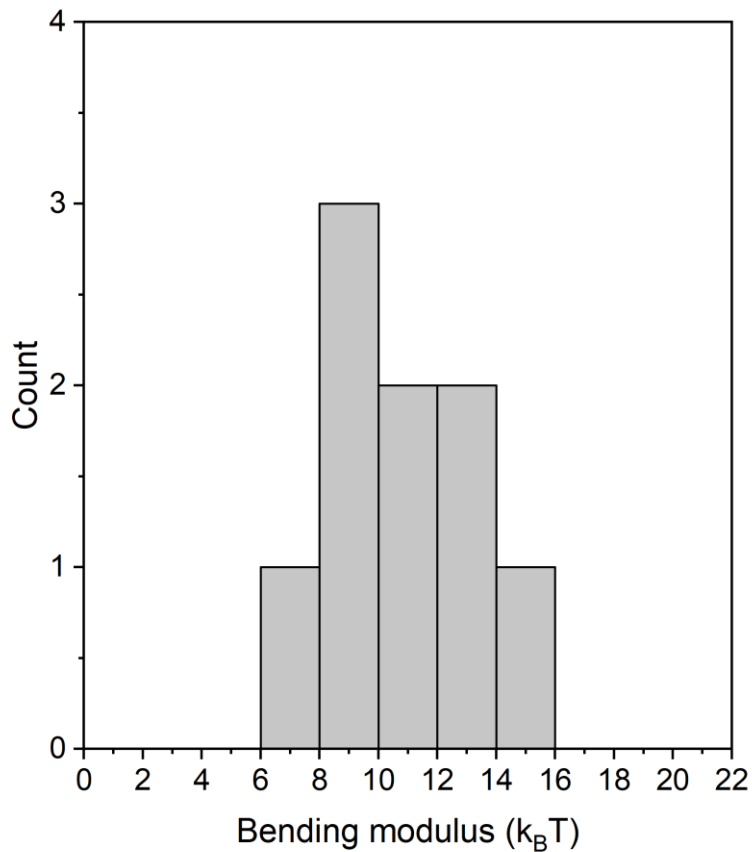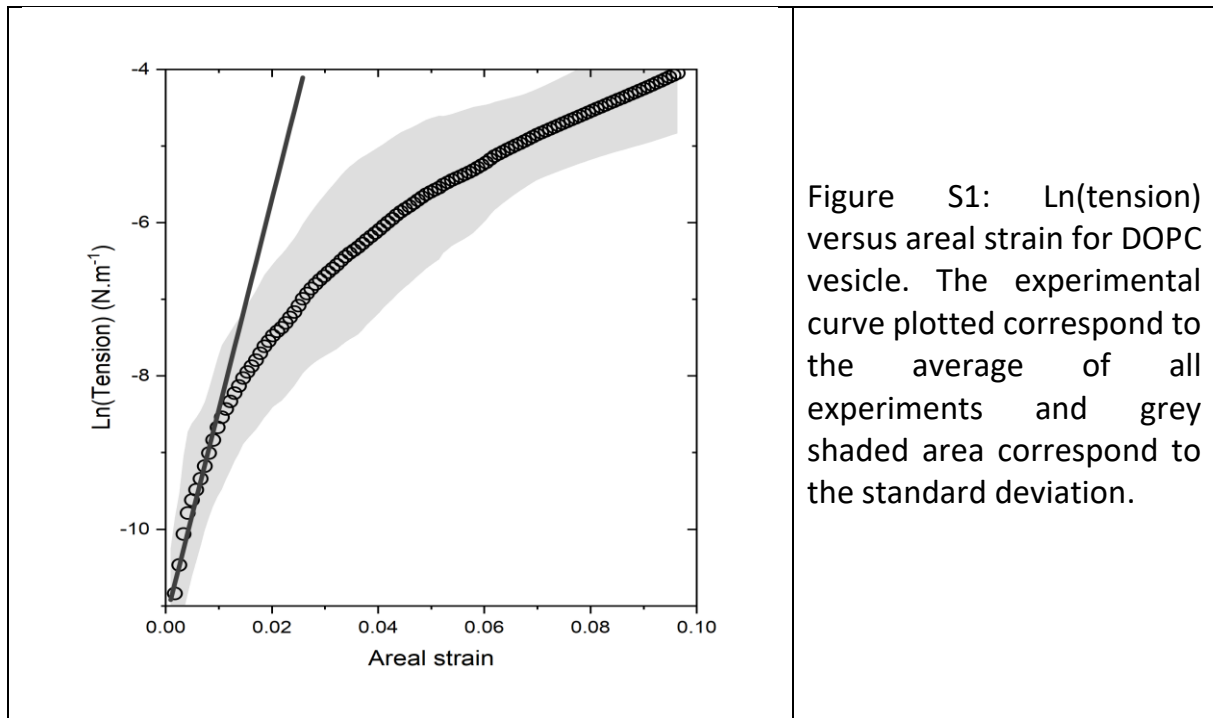

Figure S2: Histogram of the values of Kb obtained on eleven DOPC vesicles.

Calculation of relative error on line tension

The final expression of the line tension is:

$$\lambda = (h - h_0)\,\rho\,g\,\frac{R_b^2 R_p \sin\phi_1}{2(R_b - R_p \sin\phi_1)}(\cot\phi_1 - \cot\phi_2)$$

We estimate the absolute error associated to the measurement to be:

$$\Delta h = 1 \text{ μm for } h \text{ and } h_0$$
$$\Delta R = 0.5 \text{ μm for } R_b \text{ and } R_p$$
$$\Delta\Phi = 5° \text{ for } \Phi_1 \text{ and } \Phi_2$$

The relative error on line tension is:

$$\frac{\Delta\lambda}{\lambda} = \frac{\Delta h}{h} + \frac{\Delta h}{h_0} + \frac{\Delta R}{R}$$

$$\text{With } R = \frac{R_b^2 R_p \sin\phi_1}{2(R_b - R_p \sin\phi_1)}(\cot\phi_1 - \cot\phi_2)$$

$$\Delta R^2 = \left(\frac{\partial R}{\partial Rb}\right)^2 \Delta Rb^2 + \left(\frac{\partial R}{\partial Rp}\right)^2 \Delta Rp^2 + \left(\frac{\partial R}{\partial \varphi_1}\right)^2 \Delta \varphi_1^2 + \left(\frac{\partial R}{\partial \varphi_2}\right)^2 \Delta \varphi_2^2$$

$$\frac{\partial R}{\partial Rb} = RbRp\,\frac{Rb - 2Rp\sin\varphi_1}{2(Rb - Rp\sin\varphi_1)^2}\sin\varphi_1(\cot\varphi_1 - \cot\varphi_2)$$

$$\frac{\partial R}{\partial Rp} = \frac{Rb^3 \sin\varphi_1(\cot\varphi_1 - \cot\varphi_2)}{2(Rb - Rp\sin\varphi_1)^2}$$

$$\frac{\partial R}{\partial \varphi_1} = \frac{Rb^2 Rp[Rp - Rb(\sin\varphi_1 + \cos\varphi_1 \cot\varphi_2)]}{2(Rb - Rp\sin\varphi_1)^2}$$

$$\frac{\partial R}{\partial \varphi_2} = \frac{Rb^2 Rp[Rp - Rb(\sin\varphi_1 + \cos\varphi_1 \cot\varphi_2)]}{2(Rb - Rp\sin\varphi_1)^2}$$

We can estimate for a couple of values of h, h_0, R_b, R_p, Φ_1 and Φ_2 the relative error for the line tension. For example, with $\Phi_1 = 116°$, $\Phi_2 = 64°$, $R_p = 7.9$ μm, $R_b = 11$ μm, $h_0 = 5$μm, $h = 53$ μm

$$\frac{\Delta\lambda}{\lambda} = 0.47$$

The relative error is indeed quite large, which is consistent with the experimental error bar obtained.

Statistical tests on experimental values of line tension.

We performed statistical tests on the collected data to gain insight into the significance of the line tension values obtained.

A normality test (Kolmogorov-Smirnov test) was first performed. It showed a normal distribution of the data allowing parametric tests to be performed.

A one-way ANOVA test assuming non-equal standard deviation values (Brown-Forsythe and Welch test) was performed to compare the line tension obtained for the three different systems (Games-Howell's multiple comparisons post-test). These tests yielded adjusted p-values of 0.0532 and 0.0791 comparing the line tension of $PDMS_{23}$-b-PEO_{13} with that of PEO_8-b-$PDMS_{22}$-b-PEO_8 and $PDMS_{27}$-b-PEO_{17} respectively. This means that difference of line tension observed for these systems tends to be significant, considering a limit p-value of 0.05 and below to be significant. A p-value of 0.8717 was found comparing the line tension PEO_8-b-$PDMS_{22}$-b-PEO_8 with that of $PDMS_{27}$-b-PEO_{17}. Therefore, the values are significantly similar. This confirm the architecture effect of the block copolymer, the line tension being similar between a diblock and a triblock despite their high difference in hydrophobic length mismatch (~3nm).

Based on the number of values for each system, the representation of the error bars corresponds to Standard Error of Mean (SEM). P-values were added in figure 5 to visualize the significance of the difference in the line tension values.

Comparing bending energy to boundary energy

We follow the same methodology of the model proposed by Bengham and published in PR.L. in 2007[1], in which bending stiffness were neglected. We indeed verified the bending energy of a vesicle (sphere) which is [2]

$$F_{sph} = 8\pi Kb \left(1 - \frac{R}{R_{sp}}\right)^2 + 4\pi\bar{k}$$

Assuming no spontaneous Curvature R_{sp}~∞ , then

$$F_{sph} = 8\pi Kb + 4\pi\bar{k}$$

Where $\bar{k}$ is the gaussian bending modulus.

As part of the vesicle is aspirated in the pipette, we have considered also the bending energy of the tongue :

For a cylinder of radius R_0 and lenght L, with hemisphere of same radius R_0 the bending energy is :

$$F_{cyl} = \frac{\pi KbL}{R_0} + 4\pi\bar{k}$$

Typically, considering the lenght L of the tongue we obtained, a maximum of $L/R_0{\sim}4$ can be reasonably considered.

Therefore, assuming that the term implying gaussian modulus is negligible, the curvature energy of the cylinder is still below the one of the sphere, and the assumption of the model (bending energy well below the boundary energy) is still valid.

(1)   Tian, A.; Johnson, C.; Wang, W.; Baumgart, T. *Phys. Rev. Lett.* **2007**, *98*, 208102.
(2)   Jung, H. T.; Lee, S. Y.; Kaler, E. W.; Coldren, B.; Zasadzinski, J. A. *Proc. Natl. Acad. Sci.* **2002**, *99*, 15318.